J Herbmed Pharmacol. 2026; 15(1): 135-147.

http://www.herbmedpharmacol.com doi: 10.34172/jhp.2026.52879

Journal of Herbmed Pharmacology

Molecular docking and dynamics simulation of milk kefir metabolites as potential estrogen receptor alpha (ER-α) modulators for breast cancer therapy

Ivan Andriansyah[1*], Salwaa Susilo[1], Soni Muhsinin[2], Ellin Febrina[3], Widhya Aligita[4], Aiyi Asnawi[1]

[1]Department of Pharmacochemistry, Faculty of Pharmacy, Universitas Bhakti Kencana, Jl. Soekarno-Hatta No. 754, Bandung 40617, Indonesia
[2]Department of Pharmaceutics and Pharmaceutical Technology, Faculty of Pharmacy, Universitas Bhakti Kencana, Jl. Soekarno-Hatta No. 754, Bandung 40617, Indonesia
[3]Department of Pharmacology and Clinical Pharmacy, Faculty of Pharmacy, Universitas Padjadjaran, Jl. Raya Bandung-Sumedang km. 21, Jatinangor 45363, Indonesia
[4]Department of Pharmacology and Clinical Pharmacy, Faculty of Pharmacy, Universitas Bhakti Kencana, Jl. Soekarno-Hatta No. 754, Bandung 40617, Indonesia

ARTICLE INFO

Article Type:
Short Communication

Article History:
Received: 21 Dec. 2024
Revised: 22 Sep. 2025
Accepted: 30 Sep. 2025
epublished: 1 Jan. 2026

Keywords:
Breast cancer
Estrogen receptor alpha
Milk kefir
Molecular docking
Molecular dynamics

ABSTRACT

Introduction: Milk kefir, a fermenting milk made with kefir grains, has shown potential in promoting apoptosis, regulating the cell cycle, and reducing tumor growth in breast cancer cells. This study aimed to investigate the stability and potential of milk kefir metabolites as inhibitors of breast cancer growth by interacting with the estrogen receptor alpha (ER-α), a key protein involved in breast cancer cell proliferation. We used computational methods, specifically molecular docking simulations with AutoDock and molecular dynamics (MD) simulations with Gromacs, to analyze how these metabolites bind to ER-α.

Methods: A combination of molecular docking and MD simulations was used to explore how metabolites derived from milk kefir interact with ER-α, a crucial target in breast cancer therapy. The methodology included multiple stages: preparation of target proteins, preparation and screening of the metabolites, geometry optimization, molecular docking, and MD simulations.

Results: The molecular docking simulations of 43 metabolites revealed three promising candidates: 2-Methyl (S35), benzeneethanol (S42), and 2,6-dimethyl-4-heptanone (S54), with binding affinities (ΔG) of -5.08, -5.06, and -4.90 kcal/mol, respectively. MD simulations further showed that the selected metabolites stabilized the ER-α-metabolite complex, with the 2,6-dimethyl-4-heptanone (S54) metabolite demonstrating the most negative total MM-GBSA energy value (ΔG = -22.98 kcal/mol), indicating a strong and stable binding interaction.

Conclusion: 2,6-Dimethyl-4-heptanone, a metabolite from milk kefir, showed promising potential as a candidate for further development as a breast cancer treatment, offering a novel alternative to conventional therapies.

Implication for health policy/practice/research/medical education:
This study highlighted the potential of milk kefir metabolites, particularly 2,6-dimethyl-4-heptanone, as novel inhibitors for breast cancer treatment by targeting the estrogen receptor alpha (ER-α). The use of computational methods like molecular docking and molecular dynamics (MD) simulations provided a more efficient and cost-effective approach to drug discovery, especially for natural metabolites. This study also opened avenues for further exploration of natural metabolites as potential cancer therapies. Future research could focus on in vivo evaluation and clinical trials to validate the efficacy of 2,6-dimethyl-4-heptanone and similar metabolites in breast cancer treatment.

Please cite this paper as: Andriansyah I, Susilo S, Muhsinin S, Febrina E, Aligita W, Asnawi A. Molecular docking and dynamics simulation of milk kefir metabolites as potential estrogen receptor alpha (ER-α) modulators for breast cancer therapy. J Herbmed Pharmacol. 2026;15(1):135-147. doi: 10.34172/jhp.2026.52879.

***Corresponding author**: Ivan Andriansyah,
Email: ivan.andriansyah@bku.ac.id

Introduction

Breast cancer is one of the leading causes of death worldwide, accounting for 13% of deaths from non-communicable diseases (1). It arises from the loss of normal cellular control mechanisms, resulting in abnormal and uncontrolled cell proliferation (2). According to GLOBOCAN 2020, there were 2.3 million new cases and 683,000 deaths from breast cancer globally. In Indonesia, the number of cases in 2020 reached 65,858 (16.6%), with 22,430 deaths (9.6%). These numbers are projected to increase to 88,288 cases by 2050 (3). Alarmingly, nearly 70% of cancer patients in Indonesia are diagnosed at advanced stages, making breast cancer the second leading cause of death after lung cancer (4).

Traditional treatments for breast cancer, including chemotherapy, radiotherapy, hormone therapy, and surgery, are commonly used but have proven to be ineffective for many patients with advanced stages of the disease (5). Recent studies have focused on targeting estrogen receptor alpha (ER-α), a key protein involved in breast cancer cell proliferation, as a potential therapeutic strategy (6). Since approximately 70% of breast cancer patients are diagnosed with ER-α-positive tumors, targeting this receptor is an essential approach in developing effective therapies (7). Currently, endocrine therapies such as tamoxifen are used to block ER-α, but they come with significant side effects, including blood clots, stroke, uterine cancer, and cataracts (8). This highlights the need for safer and more effective ER-α-targeted therapies.

Given that conventional cancer treatments can cause long-term side effects, alternative therapies are becoming increasingly important. Among these alternatives, probiotic drinks such as milk kefir have gained attention. Milk kefir, a health-promoting fermented drink, is rich in probiotics and beneficial yeast. Despite its health benefits, it is not widely recognized as a therapeutic agent. Milk kefir is traditionally made by fermenting milk with kefir grains, which contain a mixture of bacteria and yeast, at a temperature of about 30 °C for 24 hours (9,10). Milk kefir is a fermented milk beverage that has shown promising results in cancer prevention. Research indicated that milk kefir modulated immune responses and prevented breast cancer in experimental models (11). Furthermore, milk kefir extract has been shown to induce apoptosis, arrest the cell cycle, and reduce tumor growth in breast cancer cells, making it a potentially viable option for the prevention or treatment of breast cancer (12). This fermented drink was considered beneficial in preventing and treating various diseases (13). However, its role in cancer therapy, particularly in relation to estrogen receptors, has yet to be fully explored.

Studies revealed that certain bioactive components in kefir, such as peptides, fatty acids, and probiotics, were capable of interacting with ER-α, disrupting its role in promoting the growth of estrogen-dependent breast cancer cells (14). These compounds were believed to either block estrogen from binding to the receptor or alter the receptor's activity, ultimately slowing down cancer cell proliferation. This finding led to increased interest in the therapeutic potential of fermented dairy products like kefir, highlighting their role in cancer prevention and treatment.

When comparing kefir metabolites to existing ER-α inhibitors like tamoxifen, it became evident that while tamoxifen had been widely used for treating estrogen receptor-positive breast cancer, it was not without significant limitations. Many patients experienced troublesome side effects, such as hot flashes, blood clot risks, and increased chances of uterine cancer (15). Additionally, long-term use of tamoxifen often led to resistance, reducing its effectiveness over time (16). In contrast, kefir metabolites, derived from natural fermentation processes, presented a promising alternative. These metabolites demonstrated a more selective modulation of the estrogen receptor, potentially offering a safer option with fewer side effects, such as reduced risks of blood clots or hormonal imbalances. This made kefir metabolites a compelling candidate for further research as a gentler, yet effective, option for hormone-related conditions.

The aim of this study was to identify and evaluate metabolites in milk kefir that exhibited a strong affinity for the ER-α and potentially inhibited breast cancer growth. By analyzing the stability of these interactions, we aimed to identify metabolites that could serve as novel candidates for breast cancer treatment.

Materials and Methods

The computational work for this study was conducted using a high-performance computer system running on Linux Ubuntu 22.04 LTS. The system was equipped with an Intel Xeon E5 2690 processor operating at 2.13 GHz, a GeForce RTX 3060 8GB graphics card, 1 TB of storage, and 32 GB of RAM. To carry out the simulations and analyses, several software packages were utilized, including AutoDock 4.2 for molecular docking, Gromacs 2023 for molecular dynamics (MD) simulations, and Avogadro for geometry optimization. Discovery Studio Visualizer (DSV) was employed to visualize the docking results.

This research utilized a combination of molecular docking and MD simulations to investigate the interaction of metabolites derived from milk kefir with ER-α, a key target in breast cancer therapy. The methodology included multiple stages: preparation of target proteins, preparation and screening of metabolites, geometry optimization, molecular docking, and MD simulations.

Preparation of the target protein

The three-dimensional structure of ER-α was retrieved from the Protein Data Bank (PDB) using the ID 3ERT (17). This structure provided the detailed atomic coordinates necessary for the study, allowing for an accurate representation of the receptor to be used in the molecular docking and dynamics simulations. The protein was cleaned using DSV (18). This step involved removing the native ligand (OHT), separating the protein from any bound molecules, and eliminating water molecules. The cleaned protein structure was saved in the PDB file format (*.pdb) for further use in docking simulations.

Preparation of the metabolites

The metabolites found in milk kefir were obtained from PubChem, with 61 identified metabolites relevant to this study. These metabolites were downloaded in 2D and 3D formats and converted to suitable file formats for docking simulations. The native ligand for ER-α, 4-hydroxy-tamoxifen (OHT), was used as a reference drug in this study. These metabolite files were initially in the *.sdf format, which was then converted to *.pdb format using Avogadro. A total of 61 metabolites were processed and prepared for docking simulations.

Filtering of the metabolites

To ensure that only suitable metabolites were selected for further analysis, the metabolites were screened using Lipinski's Rule of Five, which assesses the drug-likeness of molecules (19). This screening was performed using SCFBio and SwissADME. Out of 61 metabolites, 43 were found to meet the criteria of Lipinski's Rule, which suggested that these metabolites were more likely to exhibit good bioavailability. The size of the grid box for docking simulations was adjusted to accommodate the largest metabolite.

Geometry optimization

To ensure that each metabolite was in its most stable form, geometry optimization was performed using Avogadro (20). The optimization process involved applying force field settings, adjusting the number of steps to 10,000, and saving the optimized structure in *.pdb format. This step ensured that the metabolites were in their lowest energy conformations before docking simulations.

Validation of the docking method

The accuracy of the molecular docking method was validated by re-docking the native ligand (OHT) into the ER-α receptor. The validation process involved using AutoDock Tools (v4.2.4) to set up the docking environment. The protein was prepared by adding hydrogen atoms, assigning Gasteiger charges, and selecting the appropriate torsional flexibility of the native ligand. The re-docking process was performed with a grid box size of 54 × 50 × 54, and the root mean square deviation (RMSD) value was calculated. A validation method was considered successful if the RMSD value was less than 2 Å, indicating that the docking protocol could accurately reproduce the known binding mode of the native ligand.

Molecular docking of metabolites

After validating the molecular docking method, the molecular docking of the metabolites was performed using AutoDock 4.2 (21). The grid box size of 54 × 50 × 54 and coordinates (X = 29.279, Y = 2.402, Z = 24.288) were used for all metabolites. The docking process was carried out using a rigid docking approach, where the metabolites were allowed to rotate while the ER-α protein remained rigid. The Lamarckian genetic algorithm (LGA) was applied to perform the search with 100 conformations per metabolite, 100 GA runs, and a maximum of 2.5 million evaluations. The results were analyzed by examining the binding free energy (ΔG) and the inhibition constant (Ki) for each metabolite.

Visualization of docking results

The docking results were visualized using DSV. The output files in *.dlg format were analyzed to identify the best docking poses based on the lowest binding free energy (ΔG). The rank-1 cluster, which represents the conformation with the lowest energy, was saved in *.pdb format for further analysis. The interactions between the ligands and ER-α were visualized using 2D and 3D interaction diagrams to study non-covalent interactions such as hydrogen bonds, hydrophobic interactions, and electrostatic forces.

Molecular dynamics simulations

The top metabolites identified through molecular docking were selected for further analysis using MD simulations to assess the stability of the metabolite-ER-α complex. Gromacs 2023 was used to perform the MD simulations, which involved several key steps (22). First, the appropriate force fields were assigned to both the metabolite and the protein, and their topology was generated. Next, a simulation box was created around the complex, and solvent molecules (water) were added to the system. To mimic physiological conditions, counterions were introduced to neutralize the system. The system was then energy minimized to remove any steric clashes or unfavorable interactions.

Following energy minimization, the system underwent equilibration in both NVT (constant volume and temperature) and NPT (constant pressure and temperature) ensembles to stabilize the system. Production MD simulations were then run for 100 ns to observe the stability and interactions of the metabolite-ER-α complex over time. The results from the MD simulations were analyzed by calculating the RMSD, root mean square

fluctuation (RMSF), and MM-GBSA binding energies to evaluate the stability of the metabolite-protein interaction.

Statistical analysis

Given the computational nature of this study, inferential statistical analyses might not be directly applicable. However, we clarified the interpretation of computational results, emphasizing comparative trends and significance based on established computational standards.

Results

Evaluation of drug-likeness properties

Before analyzing inhibition, the metabolites from milk kefir were first screened using Lipinski's rule of five (Table 1). In evaluating the impact of a "maximum of one violation" on bioavailability, it was observed that

Tabel 1. Screening results of physicochemical properties of metabolites against Lipinski's rule

ID	Metabolites	Mass	H-Donor	H-Acceptors	LogP	Molecular weight (Dalton)
S01*	Acetoin	88	1	2	-0.043800	22.361797
S02*	Orotic acid	156	3	6	-1.205700	32.393200
S03*	Citric acid	192	4	7	-1.248500	37.091198
S04*	Pyruvic acid	88	1	3	-0.340000	18.316801
S05*	Lactic acid	90	2	3	-0.548200	19.316601
S06*	Uric acid	168	4	7	-1.692300	35.367802
S07*	Butyric acid	312	5	6	-0.053101	77.145782
S08	Hippuric acid	179	2	4	0.501000	46.410995
S09	Diacetyl	86	0	2	0.164400	21.361996
S10	*n*-Hexanal	100	0	1	1.765600	30.205992
S11*	Carbon dioxide	60	0	1	0.251100	13.284500
S12*	Carbonyl sulfide	60	0	1	0.251100	13.284500
S13	Acetone	58	0	1	0.595300	16.355001
S14	Ethyl acetate	88	0	2	0.569400	22.306997
S15*	1,2-Ethanediol	62	2	2	-1.029000	14.171601
S16	2,3-Butanedione	86	0	2	0.164400	21.361996
S17	Hexan-2-one	100	0	1	1.765600	30.205990
S18	2-Methylpropan-1-ol	74	1	1	0.634700	21.923798
S19	Pentan-2-ol	88	1	1	1.167300	26.588795
S20	1-Methoxy-2-propanol	90	1	2	0.013600	23.556797
S21	Butan-1-ol	74	1	1	0.778800	21.993797
S22	3-Methylbutan-1-ol	88	1	1	1.024800	26.540794
S23	Ethyl butyrate	116	0	2	1.349600	31.540989
S24*	Hexadecanoic acid	256	1	2	5.552299	77.947777
S25	Heptan-2-ol	116	1	1	1.947500	35.822788
S26	Hexan-1-ol	102	1	1	1.559000	31.227791
S27	1-Propanol	60	1	1	0.388700	17.376801
S28	2-Methyl-1-butanol	88	1	1	1.024800	26.540794
S29	3-Methyl-(s)	117	3	3	0.054300	30.449192
S30	Octanal	128	0	1	2.545800	39.439987
S31*	3-Hydroxy-2-butanone	312	5	6	-0.053101	77.145782
S32*	2-Hydroxy-ethyl ester	118	1	3	-0.069700	28.313793
S33	Nonanal	142	0	1	2.935899	44.056988
S34	Propionic acid	74	1	2	0.481000	17.926802
S35	2-Methyl	171	1	4	0.092020	40.704197
S36*	2,3-Butanediol	90	2	2	-0.252000	23.361599
S37	Heptanoic acid	13	1	2	2.041400	36.394791
S38	Iso-valeric acid	102	1	2	1.117100	27.090794

Tabel 1. Continued

ID	Metabolites	Mass	H-Donor	H-Acceptors	LogP	Molecular weight (Dalton)
S39	Ethanol	46	1	1	-0.001400	12.759801
S40	2-Heptanol	116	1	1	1.947500	35.822788
S41	3-Methyl-1-butanol	88	1	1	1.024800	26.540794
S42	Benzeneethanol	122	1	1	1.221400	37.231796
S43	3-Methylbutanal	86	0	1	1.231400	25.518991
S44	Acetaldehyde	122	1	2	1.384800	33.401295
S45*	Benzoic acid	312	5	6	-0.053101	77.145782
S46*	Carbamic acid	61	3	3	-0.376900	12.212200
S47	Dodecanoic acid	200	1	2	3.991899	59.479782
S48	1,2-Benzenedicarboxylic acid	166	2	4	1.083000	40.360600
S49*	Diethyl ester	384	0	4	6.306502	95.574974
S50	Acetic acid ethyl ester	88	0	2	0.569400	22.306997
S51	2-Heptanone	114	0	1	2.155700	34.822990
S52	2-Butanone	72	0	1	0.985400	20.971998
S53	2-Nonanone	142	0	1	2.935899	44.056988
S54	2,6-Dimethyl-4-heptanone	142	0	1	2.647700	43.916988
S55	Dimethyl sulfone	94	0	2	0.741600	20.811996
S56	Acetic acid	60	1	2	0.090900	13.309801
S57	Propanoic acid	74	1	2	0.481000	20.971998
S58	Butanoic acid	88	1	2	0.871100	22.543797
S59*	Hexanoic acid	88	1	2	-0.043800	77.145782
S60	Octanoic acid	144	1	2	2.431500	41.011787

* Metabolites that did not comply with Lipinski's rule.

compounds with no more than one violation of Lipinski's rule of five generally had a higher likelihood of exhibiting favorable bioavailability (19). However, the presence of a single violation did not necessarily preclude adequate absorption or effectiveness. Compounds with one violation often maintain sufficient bioavailability, although they could face challenges such as reduced solubility or permeability, which might limit their overall effectiveness. Thus, while a single violation indicated potential issues with bioavailability, it did not categorically exclude the compound from being a viable candidate for therapeutic use. This finding suggested that bioavailability could still be acceptable in compounds with minor deviations from Lipinski's guidelines.

Binding energy and binding interactions

The molecular docking method was validated through the process of re-docking the native ligand (OHT) into the ER-α receptor (Figure 1).

The results of the molecular docking simulation showed that all milk kefir metabolites were able to interact with the ER-α receptor (PDB ID: 3ERT) (Table 2).

Stability analysis of metabolite–receptor interactions

The metabolites with the strongest binding energies—S35, S42, and S54 were further analyzed through MD simulations, with the native ligand (OHT) used as a reference for comparison. The MD simulations were conducted using the Gromacs 2023 software to evaluate the stability of metabolite-receptor interactions within the complexes, based on RMSD, RMSF, and MM/GBSA values over 100 ns.

Analysis of structural stability

Based on the RMSD fluctuation analysis, all metabolites were able to maintain stable interactions with the ER-α receptor, except for metabolite S42 (Figure 2).

Analysis of residue flexibility

Based on the RMSF fluctuation analysis, all metabolites exhibited similar fluctuation patterns across the amino acid regions of the ER-α receptor. However, slight differences were observed—metabolite S35 showed stronger fluctuations within the amino acid range of 320–350, while OHT and metabolite S42 fluctuated more prominently in the 450–470 region (Figure 3).

MM/GBSA energy component

Based on the total energy components from the MM/GBSA analysis, all metabolites showed negative binding

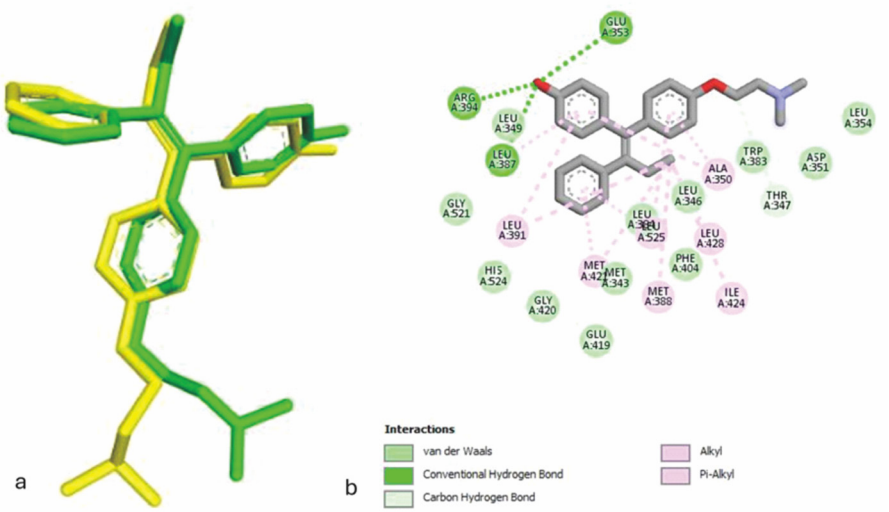

Figure 1. Comparison between the native ligand and its predicted binding conformation. (a) An overlay of the native ligand, tamoxifen (OHT), with its best-predicted binding conformation, demonstrating how closely the predicted pose aligns with the actual binding mode within the receptor's active site. (b) A 2D interaction map highlighting key molecular interactions between the native ligand and the surrounding binding site residues, providing a clearer understanding of the ligand–receptor interaction profile.

energy values, indicating favorable interactions. However, their binding energies were weaker compared to the native ligand (OHT) (Table 3).

Discussion

Evaluation of drug-likeness properties

This rule serves as a guideline to evaluate the drug-likeness of metabolites, focusing on their physicochemical properties, especially their ability to cross biological membranes (23). In this study, of a total of 61 metabolites found in milk kefir, 43 were selected for further analysis because they fulfilled the criteria of Lipinski's rule with a maximum of one violation (Table 1). The ability of a metabolite to pass Lipinski's rule is often an indicator of its potential for good absorption and bioavailability (19). By adhering to these guidelines, the metabolites that were transferred to the molecular docking stage demonstrated promising pharmacokinetic properties, suggesting that they have the potential to be effective in biological systems. The selection of these metabolites is crucial, as it ensures that only those with the highest likelihood of effective cellular permeability and oral bioavailability are

Table 2. Binding energy and inhibition constant of milk kefir metabolites

ID	Binding energy (kcal/mol)	Inhibition constant (mM)	Amino acid residue
S08	-4.00	1.16	GLU353, ARG394, LEU346, MET388
S09	-3.67	2.03	LYS449
S10	-4.05	1.08	LYS449, PRO324
S013	-3.15	4.97	ILE424, GLU423, MET421
S014	-3.50	2.72	ILE326, GLU353, LEU327, LEU349
S16	-3.68	1.99	LYS449
S17	-4.22	0,80	LYS449, HIS356,PRO324
S18	-3.45	2.95	GLU353, ALA350,LEU349, LEU346, PHE404, LEU391, ARG394
S19	-3.74	1.82	GLU353, ARG394, ALA350, LEU349,LEU387, LEU391
S20	-2.85	8.14	GLU353, ARG394, LEU396, LEU391, LEU387
S21	-3.19	4.62	ARG394, GLU353, LEU349, LEU346, PHE404
S22	-3.74	1.81	GLU353, ARG394, LEU349
S23	-3.95	1.26	LYS449, LEU387, MET357, PRO324
S25	-4.40	0,59	GLU353, ILE386, MET357, PRO324, TRP360
S26	-3.82	1.58	GLU353, ARG394, LEU346, LEU349
S27	-2.88	7.76	GLU353, LEU327, ILE326
S28	-3.73	1.86	ARG394, GLU353, ALA350, LEU346, LEU349

Tabel 2. Continued

ID	Binding energy (kcal/mol)	Inhibition constant (mM)	Amino acid residue
S29	-4.50	0,50	GLU353, LEU349, ALA350, LEU346
S30	-3.93	1.31	ARG394, LEU387, MET388, LEU525, LEU384, HIS524, LEU391
S33	-4.55	0,45	LEU32, ILE386, MET357, TRP360, PRO324
S34	-2.77	9.27	PRO324, MET357
S35	-5.08	0,18	LYS449, GLU353, PRO324, MET357, LEU327
S37	-4.04	1.10	LYS449, PRO324, HIS356
S38	-3.54	2.55	LYS449
S39	-2.69	10.59	ILE424, GLY420, LYS520
S40	-4.31	0,68	GLU353, ARG394, MET357, PRO324
S41	-3.74	1.83	GLU353, ARG394, LEU349, LEU346
S42	-5.06	0,19	GLU353, ARG394, PRO324, MET357
S43	-3.72	1.87	LYS449, PRO324
S44	-4.23	0,78	ILE386, LYS449, PRO324
S47	-4.34	0,65	ARG394, GLU353, ILE424, MET388, MET421, LEU384, LEU525
S48	-4.40	0,59	GLU353, LYS449, ILE386, PRO324
S50	-3.50	2.72	ILE326
S51	-4.50	0,50	ARG449, PRO324
S52	-3.42	3.11	LYS449
S53	-4.65	0,38	LYS449, PRO324
S54	-4.90	0,25	ARG394, LEU349, MET388, LEU387, LEU391
S55	-3.64	2.16	LYS449
S56	-2.49	14.87	ILE424, GLY420
S57	-2.77	9.30	MET357, PRO324
S58	-3.12	5.17	LYS449, PRO324, MET357
S60	-3.93	1.31	LYS449, LEU327, PRO324
Tamoxifen, OHT*	-11.69	2.71 nM	ARG394, GLU353, MET388, MET421, LEU428, ILE424, LEU525, LEU384

* Tamoxifen (OHT) was used as the native ligand and reference drug.

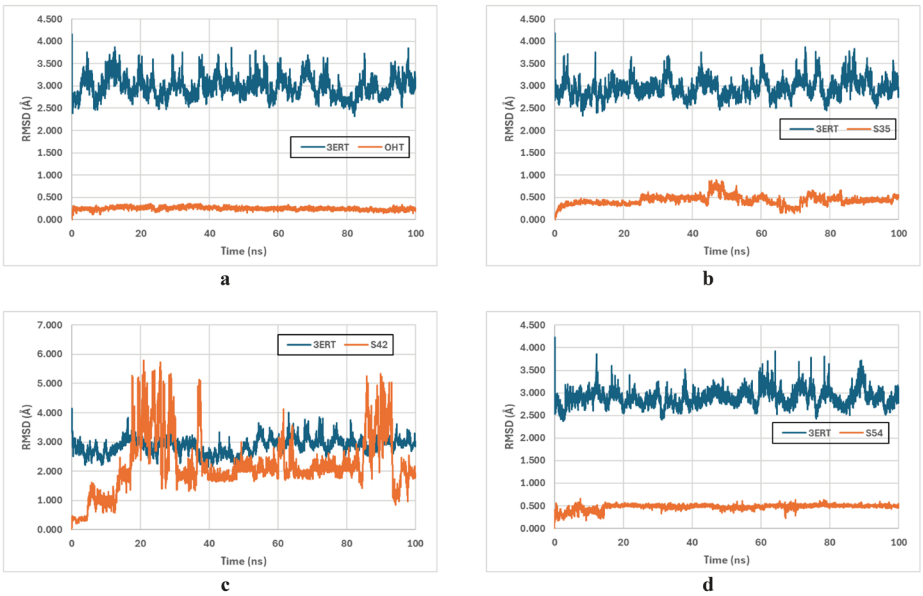

Figure 2. Root mean square deviation (RMSD) fluctuations of the native ligand and the top three hits during the 100 ns MD simulation. (a) The native ligand, OHT; (b) S35; (c) S42; (d) S54.

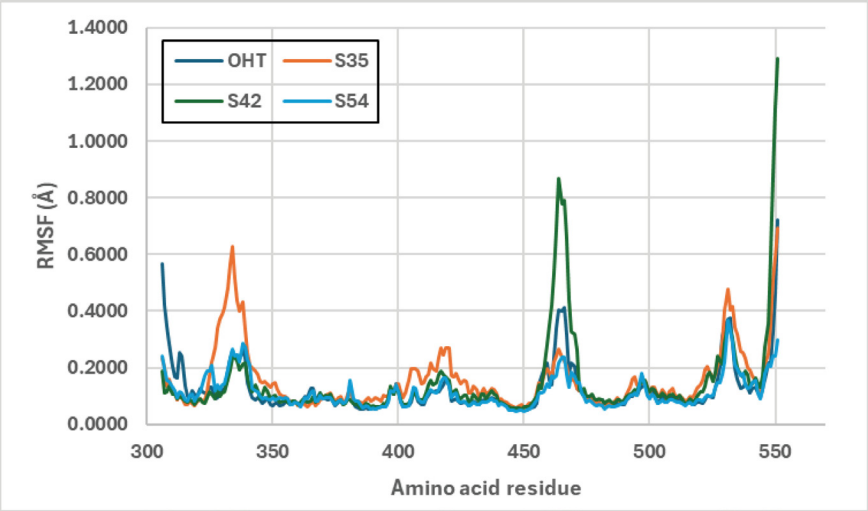

Figure 3. Residue fluctuations around the binding site, showing changes in the flexibility of the amino acid residues in ER-α during MD simulation. The native ligand and the metabolites S35, S42, and S54 were colored blue, orange, green, and light blue, respectively. RMSD: Root mean square deviation; OHT: Native ligand.

considered for the more computationally intensive steps of molecular docking and dynamics simulation.

Binding energy and binding interactions

The molecular docking method was performed by comparing the predicted ligand pose with the experimentally determined pose of the native ligand (OHT) into the ER-α receptor (17). The results showed an RMSD value of 1.239 Å, indicating a minimal deviation between the two poses. This small RMSD value suggested that the docking simulation accurately predicted the binding pose of the native ligand, further confirming the reliability of the computational model in replicating experimental findings. The binding energy of the native ligand-ER-α complex was calculated to be -11.69 kcal/mol, with a Ki of 2.71 nM, which was consistent with the known potency of OHT as a modulator of ER-α. These results further validated the docking process, confirming that the method can accurately predict binding affinities and inhibitor potency. These intermolecular interactions were essential for the stability and specificity of the native ligand binding to the receptor. In particular, the formation of hydrogen bonds between the native ligand and the receptor was crucial to the high binding affinity of OHT, as it allowed for a precise fit within the active site of the receptor. The interaction involved 21 amino acid residues at the active site of the protein, which confirmed the biological relevance of the result of the docking.

Based on these findings, the molecular docking validation was deemed successful, as the re-docking of the native ligand produced results consistent with experimental data. This served as a solid foundation for proceeding with the docking of metabolites derived from milk kefir, providing confidence in the ability of the docking approach to identify promising candidates for further investigation. Molecular docking was used to investigate the binding interactions between milk kefir-derived metabolites and the ER-α protein, to identify potential candidates that could serve as inhibitors for breast cancer. The docking results provided valuable information on the binding affinities, inhibition constants, and specific amino acid residues involved in the interaction between each metabolite and the receptor.

The binding energies of the metabolites varied, with values ranging from -2.85 kcal/mol to -4.40 kcal/mol, indicating that some metabolites demonstrated stronger binding to ER-α than others. For the metabolites with the most negative binding energies (Table 2), the structural

Table 3. The energy components associated with the binding of milk kefir metabolites to estrogen receptor alpha during the molecular dynamics simulation

	Energy component (kcal/mol)						
Metabolite	**ΔVDW**	**ΔE_{EL}**	**ΔE_{GB}**	**ΔE_{SURF}**	**ΔG_{GAS}**	**ΔG_{SOLV}**	**ΔTOTAL**
OHT	-56.10	-5.90	16.06	-7.82	-62.00	8.24	-53.76
S35	-24.41	-3.33	10.53	-3.28	-27.74	7.25	-20.49
S42	-8.60	-1.09	4.18	-1.34	-9.69	2.84	-6.86
S54	-24.73	-1.64	6.84	-3.45	-26.37	3.39	-22.98

ΔVDW: Van der Waals (ΔVDW); EEL: Electrostatic energy; ΔEGB: Electrostatic solvation energy; ΔESURF: Surface area energy; ΔGGAS: Gas-phase energy; ΔGSOLV: solvation energy; ΔTOTAL: Total free energy. These components helped evaluate the binding efficiency and thermodynamic stability of the metabolite-receptor complexes.

characteristics of the metabolites S35, S42, and S54 appeared to play a significant role in influencing their binding energies. S35 (2-methyl) showed the strongest binding affinity with a binding energy of -5.08 kcal/mol, possibly due to its compact structure that allowed better fitting into the binding site. S42 (benzeneethanol) followed closely with a slightly higher energy of -5.06 kcal/mol, which might have been influenced by the aromatic ring contributing to π-π interactions or hydrophobic contacts. Meanwhile, S54 (2,6-dimethyl-4-heptanone) exhibited the weakest interaction at -4.90 kcal/mol; its longer, branched structure might have resulted in less optimal orientation or steric hindrance within the active site. These findings suggested that smaller or more structurally compatible molecules tended to form more stable interactions in the docking process.

Based on the molecular docking results, the interaction between the metabolites and the amino acid residues of the target protein appeared to be influenced by the structural properties of each compound. S35 (2-methyl) interacted with five residues, including LYS449 and GLU353, which are polar and charged, suggesting that its small and simple structure allowed it to fit well and form contacts in both polar and hydrophobic regions of the binding site (24,25). S42 (benzeneethanol) shared some common residues with S35, such as GLU353 and PRO324, but also formed a specific interaction with ARG394, indicating that its aromatic ring and hydroxyl group might have facilitated both hydrogen bonding and π-related interactions. Meanwhile, S54 (2,6-dimethyl-4-heptanone) interacted primarily with hydrophobic residues like LEU349, LEU387, and LEU391, reflecting how its larger, branched, and more hydrophobic structure preferred nonpolar regions, potentially limiting its interaction with polar or charged residues. These differences highlighted how variations in molecular size and functional groups influenced the specificity and nature of amino acid interactions during docking.

The amino acid residues identified in the docking results, including GLU353, ARG394, LYS449, PRO324, and LEU349, play a critical role in metabolite binding. These residues were located at the active site of the receptor and participated in various intermolecular interactions, such as hydrogen bonding, van der Waals forces, and hydrophobic interactions, which stabilized the metabolite-receptor complex. The presence of these residues in multiple metabolites highlighted their importance in maintaining the stability of the metabolite-receptor interaction, making them potential targets for the design of more effective inhibitors.

In summary, the molecular docking results demonstrated that several milk kefir metabolites interacted with ER-α with varying strengths, and S35 showed the most promising binding affinity. These findings provided valuable information on the potential of milk kefir metabolites as candidates for the development of breast cancer therapies. The identified key residues involved in the metabolite-receptor interactions serve as important targets for further optimization and design of more potent inhibitors.

Based on the results of MD simulations of interactions between ER-α receptors with the metabolites, the ΔG and Ki values of the metabolites with codes S35, S42, and S54 provided the best interaction values of -5.08 and 0.18; -5.06 and 0.19; -4.9 and 0.25. The best results from the molecular docking were then proceeded to the MD simulation stage.

Stability analysis of metabolite–receptor interactions

MD simulations were conducted on the best metabolites from the molecular docking results, namely S35, S42, and S54. MD simulations were carried out using the Gromacs application to evaluate the stability of the complex (RMSD, RMSF, and MMGBSA) (26-30).

Analysis of structural stability

The RMSD graph of the native ligand showed that its structure remained relatively stable throughout the simulation, with no significant fluctuations or spikes, indicating consistent binding to the receptor. This stability suggested that the native ligand maintained a steady interaction with the receptor over time, which is favorable for sustained biological activity. In contrast, the protein's RMSD graph exhibited an initial spike within the first 7 ns of the simulation, followed by stabilization at around 17 ns, which continued for the remainder of the simulation. This fluctuation was expected in MD simulations, as the protein undergoes initial adjustments to accommodate the metabolite binding, but it quickly reached a stable conformation.

For the S35 metabolite, the RMSD graph showed an initial spike, followed by a period of stability starting at 8 ns, where the RMSD of the metabolite remained relatively constant for the rest of the simulation. This stability suggested that S35 formed a stable complex with ER-α, and its binding did not induce significant changes in the structure of the metabolite over time. But, the S42 metabolite showed more dynamic behavior. The RMSD graph for S42 showed a significant spike between 4 ns and 37 ns, followed by a period of stability. However, at 85 ns, another spike occurred, indicating that the metabolite underwent some degree of conformational change or adjustment in its binding position on the receptor. The fluctuations in the RMSD values for S42 suggested that the metabolite might have experienced difficulty in finding a stable binding pose on the receptor during the simulation. However, the S54 metabolite exhibited a relatively constant RMSD graph from the beginning of the simulation until the end. The RMSD values for both the metabolites and the protein remained below 2.0 Å and 5.0

Å, respectively, indicating that the metabolite maintained a stable interaction with the receptor throughout the 100 ns of simulation. This was a positive sign of effective and stable binding, suggesting that S54 could be a promising candidate for further evaluation.

Overall, based on the RMSD analysis, the two complexes, S35 and S54, showed the most stable interactions, with their RMSD values indicating that the metabolites remained bound to the receptor without significant structural deviations. These results suggested that S35 and S54 could be strong candidates for further investigation as potential inhibitors of ER-α in the context of breast cancer therapy. On the contrary, S42 exhibited more fluctuating behavior, which indicated that further optimization was needed to enhance its binding stability. In conclusion, the RMSD analysis provided valuable insights into the stability of metabolite-receptor complexes, with S35 and S54 being the most promising candidates for stable binding to ER-α, potentially serving as effective breast cancer drug candidates.

Analysis of residue flexibility

RMSF analysis provided crucial information on the flexibility of amino acid residues in the ER-α during the MD simulation. From the RMSF results (Figure 3), several amino acid residues exhibited high or unstable values, which were marked with red circles. These residues included ALA307, THR334, SER464, LYS531, and ALA551. The high RMSF values for these residues indicated that they were more flexible and underwent significant movement during the MD simulation. Such residues, often located in regions with less structural rigidity, were likely to experience changes in position as the protein adjusts to the metabolite binding. These regions, especially in the helical sections of the protein, lack hydrogen bonds that could otherwise help stabilize their structure, leading to increased flexibility and movement during the simulation.

On the other hand, some residues displayed low RMSF values, indicating stability during the simulation. These stable regions were included GLU353 and ARG394. The low RMSF values of these residues suggested that they were involved in stable interactions with the metabolites. Because these residues remained relatively fixed in their positions, they likely played an important role in the metabolite-binding process, maintaining the integrity of the metabolite-receptor interaction throughout the simulation. The stability of these residues suggested that they were part of the active site of the protein, where the metabolite was bound, and their minimal movement indicated that the interaction was stable and reliable.

Further analysis of the three complexes—S35, S42, and S54—revealed that the active site residues, which were crucial for metabolite binding, remained stable throughout the simulations. These residues, including GLU353 and ARG394, exhibited RMSF values <2 Å, confirming that they maintained their positions and did not undergo significant fluctuations during the simulation (31,32). This level of stability in the active site suggested that the metabolites in these complexes interacted with the receptor consistently and stably.

In conclusion, the RMSF analysis highlighted the dynamic behavior of various residues in the ER-α protein, with S35, S42, and S54 exhibiting stable binding interactions. The stable RMSF values observed for the active site residues underscore the potential of these metabolites to form stable and reliable complexes with ER-α, suggesting that they could serve as promising candidates for further investigation in the context of breast cancer treatment. The stability of key amino acids such as GLU353 and ARG394 further supported the notion that these metabolites maintain strong and stable interactions with the receptor, which was crucial for their potential therapeutic efficacy.

MM/GBSA energy component analysis

Based on Table 3, the energy components associated with the binding of milk kefir metabolites to ER-α were analyzed to understand the strength and stability of the metabolite-receptor interactions. This analysis involved several energy terms, including van der Waals (ΔVDW), electrostatic energy (ΔEEL), electrostatic solvation energy (ΔEGB), surface area energy (ΔESURF), gas-phase energy (ΔGGAS), solvation energy (ΔGSOLV), and the total free energy (ΔTOTAL) (33). These components helped evaluate the binding efficiency and thermodynamic stability of the metabolite-receptor complexes.

The ΔVDW for the native ligand (OHT) was estimated at –56.10 kcal/mol, indicating strong attractive interactions between the native ligand and the receptor. The ΔEEL was -5.90 kcal/mol, reflecting favorable electrostatic interactions that support the stability of the complex. However, the ΔEGB was positive (16.06 kcal/mol), indicating some unfavorable energy contribution from solvation effects. The ΔESURF was negative (-7.82 kcal/mol), contributing to the stability of the native ligand binding by compensating for solvation effects. The ΔTOTAL of the native ligand complex was -53.76 kcal/mol, suggesting that the native ligand binds strongly to ER-α, with a favorable overall free energy change.

For metabolite S35, the energy components were somewhat less favorable compared to the native ligand. The ΔVDW was -24.41 kcal/mol, which was significantly lower than that of the native ligand, indicating weaker van der Waals interactions. The ΔEEL was also less negative (-3.33 kcal/mol), suggesting that electrostatic interactions were not as strong. The ΔGSOLV was 7.25 kcal/mol, which was higher than the native ligand's solvated energy, indicating less favorable solvation effects. Overall, the ΔTOTAL for the S35 complex was -20.49 kcal/mol,

indicating a less stable complex compared to the native ligand but still showing favorable binding.

In the case of S42, the interaction with ER-α was less overall favorable. The ΔVDW was -8.60 kcal/mol, which was much lower than both the native ligand and the other metabolites, suggesting weaker interaction forces between the metabolite and the receptor. The ΔEEL was also less negative (-1.09 kcal/mol), and the ΔEGB was relatively small (4.18 kcal/mol). The ΔTOTAL for S42 was -6.86 kcal/mol, indicating that this metabolite had the weakest binding affinity to ER-α among the metabolites.

Finally, for S54, the ΔVDW was -24.73 kcal/mol, indicating a strong interaction between the metabolite and the receptor. The ΔEEL was -1.64 kcal/mol, and the ΔEGB was 6.84 kcal/mol, both contributing to the overall stability of the complex. The ΔTOTAL for S54 was -22.98 kcal/mol, reflecting a relatively strong and stable binding, similar to that of the native ligand.

In conclusion, the analysis of the energy components revealed that the OHT had the most favorable energy profile, with a strong overall binding affinity to ER-α. Among the metabolites, S54 demonstrated the most promising binding with an energy profile similar to that of the native ligand, while S35 showed a moderate binding affinity. On the other hand, S42 showed a weaker binding affinity, with less favorable energy components. These findings suggested that S35 and S54 were potential candidates for further investigation, as they exhibit relatively strong and stable interactions with the ER-α, which made them promising metabolites for the development of anti-breast cancer drugs. Since the current outcomes are restricted to in silico analyses, they should be interpreted with caution. Further validation through well-designed in vitro and in vivo experiments will be essential to substantiate these findings and explore their translational potential.

Conclusions

This study provided an overview of the molecular modeling of milk kefir metabolites as potential candidates for breast cancer treatment by targeting the ER-α receptor. Molecular docking of 43 metabolites identified three key metabolites, S35, S42, and S54, which showed strong interactions with the ER-α receptor, with binding energies of -5.08, -5.06, and -4.90 kcal/mol, respectively. MD simulations demonstrated that these metabolites, particularly S54, exhibited stability and interactions similar to the native ligand, suggesting their potential to stabilize the complex. RMSD, RMSF, and hydrogen bond stability analyses further supported that both OHT (the reference drug) and metabolites S35 and S54 were able to stabilize their respective complexes effectively. Although these findings are promising, experimental validation through in vitro and in vivo studies is needed to confirm their therapeutic potential. Future research should focus on optimizing these metabolites for improved efficacy and bioavailability, as well as conducting further testing in biological models to validate their suitability for clinical use in breast cancer therapy.

Acknowledgment

We would like to express our sincere gratitude to DRPM Universitas Bhakti Kencana for funding this research through the 2024 internal research under grant number 045/01/UBK/VII/2024. Our deepest appreciation also goes to our colleagues, mentors, and families for their continuous support and encouragement throughout this study.

Author's contribution

Conceptualization: Ivan Andriansyah.
Data curation: Salwaa Susilo and Ellin Febrina.
Formal analysis: Salwaa Susilo and Soni Muhsinin.
Investigation: Salwaa Susilo and Aiyi Asnawi.
Methodology: Aiyi Asnawi and Widhya Aligita.
Project administration: Ivan Andriansyah.
Resources: Ivan Andriansyah.
Software: Salwaa Susilo.
Supervision: Aiyi Asnawi.
Validation: Ivan Andriansyah.
Visualization: Soni Muhsinin.
Writing–original draft: Ivan Andriansyah.
Writing–review & editing: Aiyi Asnawi.

Conflict of interests

The authors affirm that there are no conflicts of interest in connection with this research.

Ethical considerations

The authors of this study confirm that all ethical issues, such as copyright infringement, plagiarism, data creation, duplicate publication, and redundancies, have been considered and resolved. No animal or human subjects have been utilized in the present study.

Funding/Support

The study was funded by the 2024 internal research grant from DRPM Universitas Bhakti Kencana, under grant number 045/01/UBK/VII/2024.

References

1. Łukasiewicz S, Czeczelewski M, Forma A, Baj J, Sitarz R, Stanisławek A. Breast cancer-epidemiology, risk factors, classification, prognostic markers, and current treatment strategies-an updated review. Cancers (Basel). 2021;13(17):4287. doi: 10.3390/cancers13174287.
2. Mir MA, Khan SU, Aisha S. Cell cycle dysregulation in breast cancer. In: Mir M, ed. Therapeutic potential of Cell Cycle Kinases in Breast Cancer. Singapore: Springer; 2023. p. 103-31. doi: 10.1007/978-981-19-8911-7_5.

3. Andinata B, Bachtiar A, Oktamianti P, Partahi JR, Dini MS. A comparison of cancer incidences between Dharmais cancer hospital and GLOBOCAN 2020: a descriptive study of top 10 cancer incidences. Indones J Cancer. 2023;17(2):119-22. doi: 10.33371/ijoc.v17i2.982.
4. Anwar SL, Avanti WS, Nugroho AC, Choridah L, Dwianingsih EK, Harahap WA, et al. Risk factors of distant metastasis after surgery among different breast cancer subtypes: a hospital-based study in Indonesia. World J Surg Oncol. 2020;18(1):117. doi: 10.1186/s12957-020-01893-w.
5. Burguin A, Diorio C, Durocher F. Breast cancer treatments: updates and new challenges. J Pers Med. 2021;11(8):808. doi: 10.3390/jpm11080808.
6. Al-Kabariti AY, Abbas MA. Progress in the understanding of estrogen receptor alpha signaling in triple-negative breast cancer: reactivation of silenced ER-α and signaling through ER-α36. Mol Cancer Res. 2023;21(11):1123-38. doi: 10.1158/1541-7786.Mcr-23-0321.
7. Tavčar Kunstič T, Debeljak N, Fon Tacer K. Heterogeneity in hormone-dependent breast cancer and therapy: steroid hormones, HER2, melanoma antigens, and cannabinoid receptors. Adv Cancer Biol Metastasis. 2023;7:100086. doi: 10.1016/j.adcanc.2022.100086.
8. Kumar S, Gupta S, Maurya AP, Singh R, Nigam S. Hormonal and targeted treatments in breast cancer. In: Sharma SC, Mazumdar A, Kaushik R, eds. Breast Cancer: Comprehensive Management. Singapore: Springer; 2022. p. 443-63. doi: 10.1007/978-981-16-4546-4_21.
9. Nejati F, Capitain CC, Krause JL, Kang GU, Riedel R, Chang HD, et al. Traditional grain-based vs. commercial milk kefirs, how different are they? Appl Sci. 2022;12(8):3838. doi: 10.3390/app12083838.
10. Aligita W, Singgih M, Sutrisno E, Adnyana IK. Hepatoprotective properties of water kefir: a traditional fermented drink and its potential role. Int J Prev Med. 2023;14:93. doi: 10.4103/ijpvm.ijpvm_29_22.
11. Soares T, da Silva BB, Araújo DS, de Figueiredo MC, das Chagas Leal Bezerra F, da Silva EA, et al. Therapeutic potential of using probiotics in the treatment and prevention of breast cancer. J Health Biol Sci. 2021;9(1):1-8. doi: 10.12662/2317-3076jhbs.v9i1.3783.p1-8.2021.
12. Sharifi M, Moridnia A, Mortazavi D, Salehi M, Bagheri M, Sheikhi A. Kefir: a powerful-probiotics with anticancer properties. Med Oncol. 2017;34(11):183. doi: 10.1007/s12032-017-1044-9.
13. Frąckiewicz J. The nutritional and health value of milk and fermented milk drinks®. Technological Progress in Food Processing. 2022(1):142-51.
14. Borella F, Carosso AR, Cosma S, Preti M, Collemi G, Cassoni P, et al. Gut microbiota and gynecological cancers: a summary of pathogenetic mechanisms and future directions. ACS Infect Dis. 2021;7(5):987-1009. doi: 10.1021/acsinfecdis.0c00839.
15. Hammarström M, Gabrielson M, Crippa A, Discacciati A, Eklund M, Lundholm C, et al. Side effects of low-dose tamoxifen: results from a six-armed randomised controlled trial in healthy women. Br J Cancer. 2023;129(1):61-71. doi: 10.1038/s41416-023-02293-z.
16. Buijs SM, Oomen-de Hoop E, Braal CL, van Rosmalen MM, Drooger JC, van Rossum-Schornagel QC, et al. The impact of endoxifen-guided tamoxifen dose reductions on endocrine side-effects in patients with primary breast cancer. ESMO Open. 2023;8(1):100786. doi: 10.1016/j.esmoop.2023.100786.
17. Shiau AK, Barstad D, Loria PM, Cheng L, Kushner PJ, Agard DA, et al. The structural basis of estrogen receptor/coactivator recognition and the antagonism of this interaction by tamoxifen. Cell. 1998;95(7):927-37. doi: 10.1016/s0092-8674(00)81717-1.
18. Adelusi TI, Oyedele AK, Boyenle ID, Ogunlana AT, Adeyemi RO, Ukachi CD, et al. Molecular modeling in drug discovery. Inform Med Unlocked. 2022;29:100880. doi: 10.1016/j.imu.2022.100880.
19. Karami TK, Hailu S, Feng S, Graham R, Gukasyan HJ. Eyes on Lipinski's rule of five: a new "rule of thumb" for physicochemical design space of ophthalmic drugs. J Ocul Pharmacol Ther. 2022;38(1):43-55. doi: 10.1089/jop.2021.0069.
20. Snyder HD, Kucukkal TG. Computational chemistry activities with Avogadro and ORCA. J Chem Educ. 2021;98(4):1335-41. doi: 10.1021/acs.jchemed.0c00959.
21. Bitencourt-Ferreira G, Pintro VO, de Azevedo WF Jr. Docking with AutoDock4. Methods Mol Biol. 2019;2053:125-48. doi: 10.1007/978-1-4939-9752-7_9.
22. Kutzner C, Kniep C, Cherian A, Nordstrom L, Grubmüller H, de Groot BL, et al. GROMACS in the cloud: a global supercomputer to speed up alchemical drug design. J Chem Inf Model. 2022;62(7):1691-711. doi: 10.1021/acs.jcim.2c00044.
23. Sun J, Rutherford ST, Silhavy TJ, Huang KC. Physical properties of the bacterial outer membrane. Nat Rev Microbiol. 2022;20(4):236-48. doi: 10.1038/s41579-021-00638-0.
24. Loladze VV, Ermolenko DN, Makhatadze GI. Thermodynamic consequences of burial of polar and non-polar amino acid residues in the protein interior. J Mol Biol. 2002;320(2):343-57. doi: 10.1016/s0022-2836(02)00465-5.
25. Tulumello DV, Deber CM. Positions of polar amino acids alter interactions between transmembrane segments and detergents. Biochemistry. 2011;50(19):3928-35. doi: 10.1021/bi200238g.
26. Asnawi A, Febrina E, Aman LO, Razi F. Exploring binding affinities of acetoacetate in acrylamide-based polymers (PAM) for molecularly imprinted polymers (MIPS): a molecular docking and molecular dynamics study. Int J Appl Pharm. 2023;15(2):101-8. doi: 10.22159/ijap.2023.v15s2.19.
27. Asnawi A, Febrina E, Aligita W, Aman LO, Razi F. Molecular docking and molecular dynamics study of 3-hydroxybutyrate with polymers for diabetic ketoacidosis-targeted molecularly imprinted polymers. J Pharm Pharmacogn Res. 2024;12(5):822-36. doi: 10.56499/jppres23.1926_12.5.822.
28. Febrina E, Regina P, Susilawati Y, Sofian FF, Asnawi A. In silico screening of *Laminaria japonica* ligands as potential inhibitors of DPP-4 for type 2 diabetes treatment. Trop J Nat Prod Res. 2025;9(1):157-67. doi: 10.26538/tjnpr/v9i1.23.
29. Ischak NI, Aman LO, Hasan H, Kilo A, Asnawi A. In silico screening of *Andrographis paniculata* secondary metabolites as anti-diabetes mellitus through PDE9 inhibition.

Res Pharm Sci. 2023;18(1):100-11. doi: 10.4103/1735-5362.363616.
30. Aman LO, Ischak NI, Tuloli TS, Arfan A, Asnawi A. Multiple ligands simultaneous molecular docking and dynamics approach to study the synergetic inhibitory of curcumin analogs on ErbB4 tyrosine phosphorylation. Res Pharm Sci. 2024;19(6):754-65. doi: 10.4103/rps.Rps_191_23.
31. Febrina E, Asnawi A. Lead compound discovery using pharmacophore-based models of small-molecule metabolites from human blood as inhibitor cellular entry of SARS-CoV-2. J Pharm Pharmacogn Res. 2023;11(5):810-22.
32. Putra PP, Asnawi A, Hamdayuni F, Arfan A, Aman LO. Pharmacoinformatics analysis of *Morus macroura* for drug discovery and development. Int J Appl Pharm. 2024;16(1):111-7. doi: 10.22159/ijap.2024.v16s1.26.
33. Valdés-Tresanco MS, Valdés-Tresanco ME, Valiente PA, Moreno E. gmx_MMPBSA: a new tool to perform end-state free energy calculations with GROMACS. J Chem Theory Comput. 2021;17(10):6281-91. doi: 10.1021/acs.jctc.1c00645.